Journal of Physics: Conference Series **312** (2011) 092005 doi:10.1088/1742-6596/312/9/092005

The Gamma Decay of the Pygmy Resonance and the Neutron Skin of Nuclei

A. Bracco

Dipartimento di Fisica dell'Università degli Studi di Milano and INFN, Sezione di Milano, Milano, via Celoria 16, Italy

Angela.Bracco@mi.infn.it

Abstract. The Coulomb excitation of the neutron rich ^{68}Ni was measured using it as as secondary radioactive beam at 600 MeV/nucleon impinging on a ^{197}Au target. The dipole strength in the region at around the nucleon binding energy was extracted from the gamma decay measurement. A sizable fraction of "pygmy" dipole strength, energetically located below the giant dipole resonance, is observed in this nucleus. The experimental data is discussed in connection with predictions obtained using different Random Phase Approximation (RPA) models for the dipole response, based on a representative set of Skyrme effective forces plus meson-exchange effective Lagrangians. A comparison with the experimental data for both ^{68}Ni and ^{132}Sn has allowed us to constrain the value of the derivative of the symmetry energy at saturation. The neutron skin radius is deduced under this constraint.

1. Introduction

The investigation of the size and properties of neutron skins in medium and heavy mass nuclei is a very interesting problem in nuclear physics because of its implications in the physics of neutron stars. Indeed neutron skins and the crust of neutron stars are both built from neutron-rich nuclear matter and therefore it becomes very appealing to study this feature of neutron rich nuclei since one-to-one correlations were drawn between neutron-skin thicknesses in nuclei [1,2] and specific properties of neutron stars. The thickness of the neutron skin depends on the pressure of neutron-rich matter: the greater is the pressure, the thicker is the skin as neutrons are pushed out against surface tension. The same pressure supports a neutron star against gravity. Thus models with thicker neutron skins often produce neutron stars with larger radii. In the work reported in reference 3 it was pointed out that the experimentally observed "pygmy" dipole (E1) strength might play an equivalent role as the neutron root mean square radius in constraining the nuclear symmetry energy. This is because the excess neutrons forming the skin give rise to pygmy dipole transitions at excitation energies below the giant dipole resonance. Presently the question to which extent in general such transitions represent a collective vibration of excess neutrons against an isospin symmetric core is theoretically under discussion [4-7].

Experimental evidence for pygmy dipole resonances (PDR) is still rather scarce, particularly for neutron rich nuclei that are becoming available at radioactive beam facilities. Stable nuclei including

N = 82 isotones and ^{208}Pb were investigated in (γ, γ') reactions [8-10] and were found to display a concentration of dipole strength below the neutron-separation threshold, absorbing, however, a much smaller fraction of the Thomas-Reiche-Kuhn sum rule as compared with that of unstable nuclei. To investigate further the nature of the dipole strength below the neutron separation energy, a very interesting work was made using the experimental technique of α-γ coincidence. This technique allows to separate the excitations of E1 nature from other excitation in the same energy region characterized by multipolarities different than one. In addition the used set up provided an excellent energy resolution. A concentration of electric-dipole excitations below the neutron or proton separation energy, namely the pygmy dipole resonance, has been found also with the α-γ coincidence in inelastic scattering with bombarding energy of 136 MeV on the ^{140}Ce nucleus [11]. Moreover, these experiments recently made also for other medium mass nuclei (see [12]) show that the pygmy dipole resonance states split into two parts with different nuclear structure: one part which is excited in (α, α'γ) as well as (γ, γ') experiments and one part which is excited only in (γ, γ'). A general feature of the strength of the E1 transions measured with the (γ, γ') technique is that is less than 1 % of the energy weighted sum rule (EWSR) strength is observed.

In the case of nuclei far from stability, as those produced as radioactive beams, the low-lying E1 strength function has been measured starting at the energy above the neutron binding energies in light neutron rich isotopes, like oxygen [13], ^{26}Ne [14], and in $^{129-132}$Sn and $^{133-134}$Sb isotopes [15,16]. For these studies the Coulomb dissociation technique of high-energy radioactive beams was used. In particular the measurements of $^{22-24}$O , $^{129-132}$Sn and $^{133-134}$Sb were made at GSI with the LAND set up and the fragment separator starting with ^{238}U at 550 MeV/ nucleon while the measurement for the nucleus ^{26}Ne was performed at RIKEN at bombarding energy of 80 MeV/nucleon. In all cases the measured E1 response function was found in the region just above the neutron binding energy to have a strength higher than that expected from the tail of the giant dipole resonance (GDR) and whose value is few percent of the strength.

The present paper reports on the study of the gamma decay of the pygmy resonance in the unstable ^{68}Ni nucleus. It is anticipated that values of the neutron skins and of derivative of the symmetry energy were obtained from the combined analysis of the ^{68}Ni results and of that for the ^{132}Sn nucleus, previously measured by the LAND collaboration.

The neutron rich ^{68}Ni nucleus represents a good case to investigate the pygmy structures being this nucleus located in the middle of the long isotopic Ni chain having at the extremes the doubly magic ^{56}Ni and ^{78}Ni. The descriptions of the used experimental technique and of data analysis to deduced the strength of pygmy resonance in ^{68}Ni are given in sections 2 and 3. The correlations between the behaviour of the nuclear symmetry energy, the neutron skins, and the percentage of the EWSR exhausted by the pygmy dipole resonance in ^{68}Ni and ^{132}Sn were examined. These correlations are found as a results of an analysis based on the use of different Random Phase Approximation (RPA) models for the dipole response. The dipole response predictions used for this analysis were obtained using a representative set of Skyrme effective forces plus meson-exchange effective Lagrangians. The comparison of the experimental data with the prediction is made to provide constrains on the value of the derivative of the symmetry energy at saturation. The neutron skin radius for ^{68}Ni, ^{132}Sn and ^{208}Pb were then deduced. These issues are presented and discussed in section 4 and conclusions and perspectives given in section 5.

2. The Experiment

The experiment measured the gamma decay of the pygmy resonance in the unstable nucleus ^{68}Ni used in inelastic scattering in inverse kinematics on a high Z target together with the detection of gamma-rays in coincidence with the particles scattered at angles smaller than that corresponding to the grazing collision. A schematic drawing of the experimental set up is shown in figure 1. The radioactive ^{68}Ni beam was produced by fragmentation of a primary ^{86}Kr beam delivered by the SIS synchrotron at GSI at 900 MeV/u and focussed on a Be target. The ^{68}Ni ions were selected and

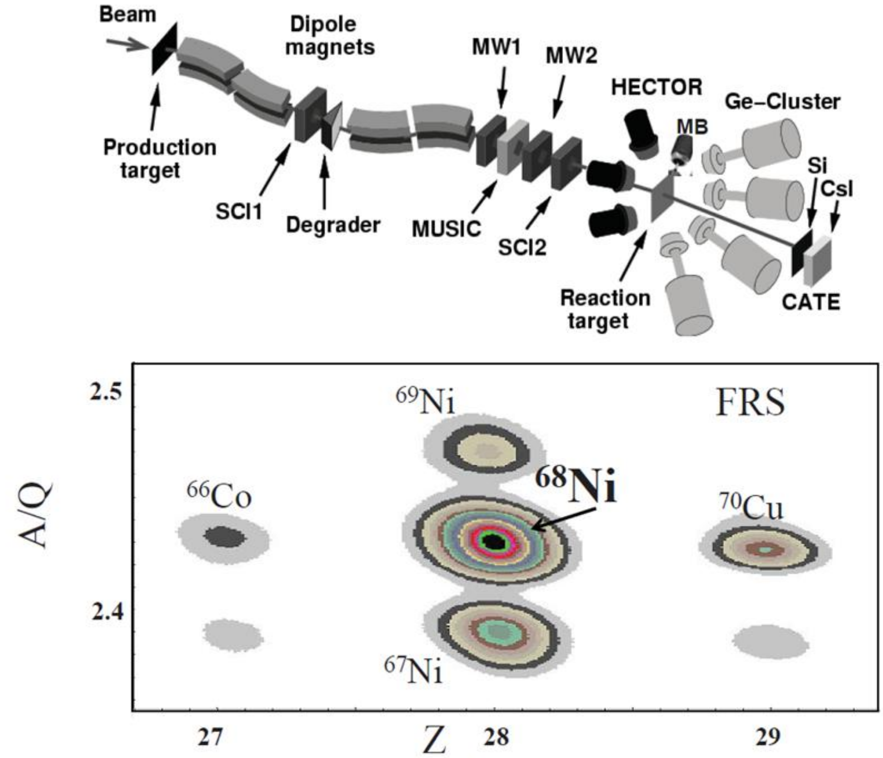

Figure 1. A schematic view of the experimental set up used for the experiment.The different gamma detectors are indicated with HECTOR (the BaF2 scintillator detectors) MB (the HPGe detectors of the miniball array) and Ge-clusters (the HPGe of Euroball). The particle detectors before the target (gas counters and scintilators) are used to identify the incident particle while the CATE calorimeteris used to identify the reaction products. In the lower panel the composition of the beam impinging on the Au target as selected with the fragment separator is shown. The A/Q versus Z plot of the ions used as a secondary beam is given and the arrow indicates the ^{68}Ni nuclei.

transported with the Fragment Separator FRS [17]. The settings of the FRS were chosen to accept secondary fragments with a magnetic rigidity corresponding to a certain mass-over-charge ratio and that provided a beam cocktail containing in large fraction ^{68}Ni ions (as one can see in the bottom panel of figure 1). The different nuclei contained in the secondary beam were identified uniquely according to their nuclear charge and mass number on an event-by-event basis. The ^{68}Ni ions constitute the most intense component (33% of the beam cocktail) impinging on a gold Au target (2g/cm^2 thick). The particle identification after the Au target was performed using the calorimeter (CATE) [18] placed at 0^{o}. This calorimeter consisted of nine thin position sensitive Si detectors placed in front of four 6 cm thick CsI scintillator detectors, arranged symmetrically with respect to the beam direction. The opening angle of the calorimeter CATE was ± 2.0^{o}, which is much larger than the grazing angle of this reaction. The grazing angle, corresponding to the maximum angle at which the interaction is strongly dominated by the Coulomb interaction is in equal to 0.43^{o}. At larger angle the contribution of hadronic interaction becomes more important and therefore also other multipoles can be excited. The total energy loss correlation of events in the CATE calorimeter corresponding to ^{68}Ni ions were measured with a resolution in mass of approximately 1%. Therefore the present resolution is sufficient to discriminate between different masses of the outgoing nuclei. The -ray emission at the target location was measured using a specific configuration of the RISING set-up [19]. Gamma rays were detected at different angles, at 16^o , 33^o , and 36^o using 15 HPGe cluster detctors of the RISING array, at 51^o and 88^o with 7 HPGe segmented cluster detectors of the Miniball array and at 88^o and 142^o with 8 BaF_2 detectors of the HECTOR array [20]. The good timing properties of the BaF_2 detectors were exploited to discriminate against gamma events originating at different locations along the beam line, using the time of flight measurement. More details are in references 21 and 22.

3. Experimental results

In figure 2 the energy spectrum of the -rays emitted in the inelastic collision of the ^{68}Ni beam on ^{197}Au target is shown. This spectrum was measured using BaF_2 scintillator detectors. The measured cross section as a function of -ray energy, shown with filled circles, is characterized by an exponential shape plus a bump at around 10-11 MeV. In order to explain the exponential part of the spectrum statistical model predictions for the gamma emission from the target and from the projectile were made and these are shown in figure 2 in comparison with the data. For statistical model calculations we have used the energy value given by the adiabatic cutoff energy of the Coulomb excitation process. The calculated statistical emission from the target and projectile was obtained using the standard GDR strength function, by correcting the -ray energy for the Doppler shift due to the projectile velocity and by folding with the detector response function. From figure 2 one can note that the sum of the target and projectile statistical contributions reproduces remarkably well the exponential shape of the data with the exception of the region where there is an excess yield, very pronounced at around 11 MeV, which can be attributed to the projectile emission on the basis of Doppler correction arguments. In addition, the width of measured bump is well reproduced by the simulation (made with the GEANT code) of the detection system response function which includes a rather large Doppler broadening dominating the energy resolution (see inset of figure 2).

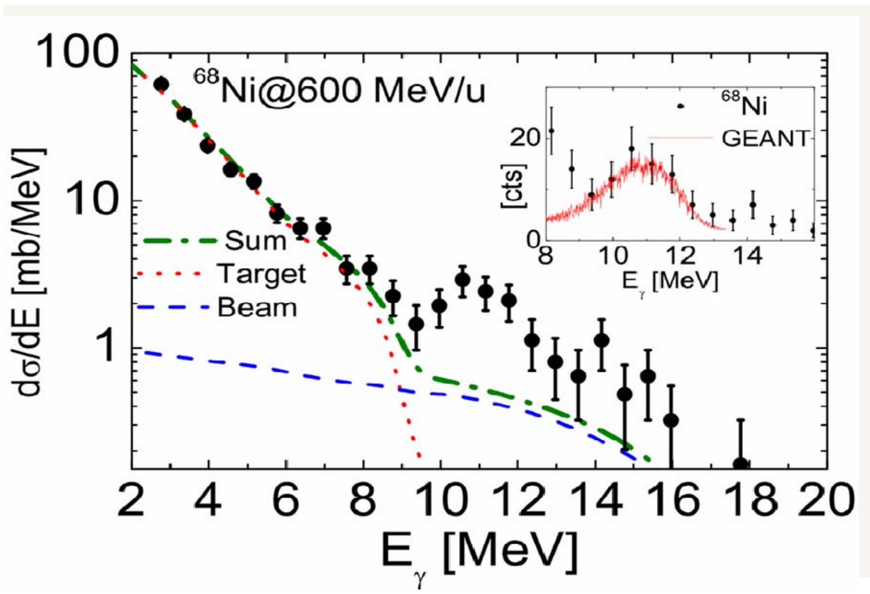

Figure 2. The high-energy -ray spectrum measured with BaF2 detectors and Doppler corrected with the velocity of the projectile. The lines are the statistical model calculations for the target (dotted line) and for the beam (dashed line) nuclei. In the inset the continuous line superimposed to the measured data is resulting from a GEANT simulation for a -transition at 11 MeV.

The data in the region of interest for the search of the pygmy resonance in the electric dipole response function were then obtained by subtracting from the measurements the computed statistical model contribution and some background extrapolated from the very high-energy region.

In figure 3 the cross section for the gamma decay of ^{68}Ni at E > 7 MeV measured with the BaF_2 detectors is shown. The measured cross section is compared with predictions obtained making different assumptions for the E1 strength function. An electric dipole response function with a small peak at 11 MeV with 5 % of the energy is added to the tail of the GDR in order to reproduced the data.

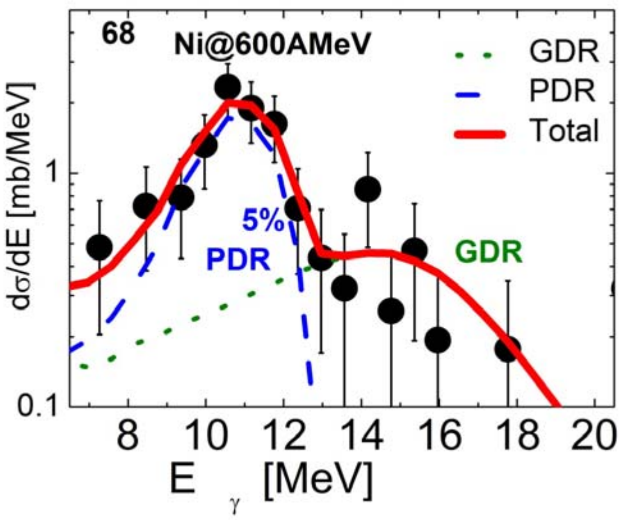

Figure 3. The measured cross section with the BaF_2 detectors is shown with filled circles (the statistical contribution was subtracted). The corresponding predictions (folded with the detector response function) are shown with lines. The long-dashed line shows the prediction when only a PDR strength is considered, the short-dashed line corresponds to the standard GDR strength without a pygmy component, and the full drawn-line is the sum of the two calculations.

In the calculation presented in figure 3 the gamma branching ratio R was calculated using as a level density that of reference 23 based on Shell Model Monte Carlo calculations. A more detailed description of these calculations which include also the computation of the virtual photon spectra is in reference 21. There is a remarkable agreement of the calculated cross section with the data (without any normalization factor) both in size and shape when one assumes an electric dipole strength function with 5% of EWSR strength at 11 MeV (the corresponding B(E1) value being 1.2 e^2fm^2).

4. Comparison with theory

Calculations of the dipole response function for the nucleus ^{68}Ni are available for different Skyrme forces. The calculation made using the RPA method and corresponding to the particular Skyrme force SkI3 [24] is shown in the left panel of figure 4. The corresponding cross section for the gamma decay is shown in the right panel of figure 4 in comparison with the experimental data. The two calculations on the right panel of figure 4 were obtained by including the gamma branching ratio and the virtual photon spectrum and the detection response function. The theoretical prediction corresponding to this specific SkI3 force reproduces reasonably well the data. However, this result has to be taken with some caution because there are several Skyrme forces available and it is difficult to claim that SkI3 is in general better than the others. In addition another theoretical approach could be used, namely the well-known relativistic mean field (RMF) theory plus the self-consistent relativistic RPA (RRPA) which has been shown to provide in general a good description of the E1 response function.

An interesting aspect of the RPA and RRPA analyses is that one can obtain information on the symmetry energy and on the neutron skin thickness associated to the specific used interactions [24]. The examination of these quantities for each specific interaction is therefore very useful to gain insight into these quantities and on their correlations. For this purpose one needs to recall the definition of relevant quantities entering into the used model and which are useful for the following discussions. The energy per particle in a nuclear system is characterized by a total density (which is equal to the sum of the neutron and proton densities $_n$ and $_p$), and by a local asymmetry • ($_n$ - $_p$)/ . In particular its expression is usually written as:

$$\frac{E}{A}(\rho,\delta) = \frac{E}{A}(\rho,\delta = 0) + S(\rho)\delta^2.$$

It should be reminded that in the above expansion odd powers of the local asymmetry density are forbidden because of the isospin symmetry while the contribution to the energy per particle given by the term proportional to ^{4} is found to be negligible. The above equation defines the so-called symmetry energy which is denoted by S( ). Presently one of the major challenges for the nuclear physics community is the determination of the values of the symmetry energy at various densities starting from those of interest for nuclear structure up to those characterizing nuclear reactions with heavy ions at different energies. The knowledge of the symmetry energy S( ) is of interest for astrophysics for the modelling of neutron stars.

The derivative of the symmetry energy at nuclear saturation density $_0$ is related to the widely used "slope" parameter L by the expression:

$$S'(\rho)\,|_{\rho=\rho_0} = \frac{L}{3\rho_0}$$

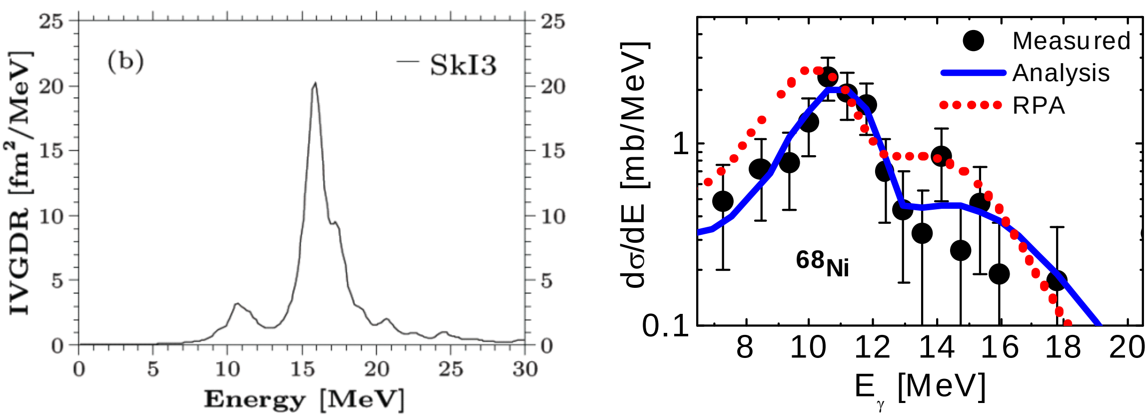

Figure 4. *Left panel*: the predicted energy distribution of the isovector dipole response function for the nucleus ^{68}Ni obtained within the RPA approach and using the Skyrme force SkI3. *Right panel*: the measured cross section of the gamma decay from ^{68}Ni in the region of the pygmy resonance is shown as a function of gamma ray energy with filled circles. The corresponding calculation including Lorentzian shape E1 distribution (as in figure 3) is shown with the full drawn line while the dotted line is the calculation using for the E1 strength function the RPA prediction shown in the left panel.

The symmetry energy at saturation S($_0$) is denoted either with a_4 or J. There is a direct correlation between the neutron skin thickness R (where R = $R_n - R_p$, namely the difference of the radius of the neutron distribution with that of the proton distribution) and the slope parameter L, as discussed in references 16 and 24. Presently the available measurements of the neutron skin thicknesses in several neutron rich nuclei give values covering a rather wide interval so that it is not possible on the base of these results to provide a good constrain for the slope parameter L.

Calculations of the dipole response function, of the "slope" parameter, and of the neutron skin thickness R were made using a wide set of Skyrme interactions which constitute a quite representative ensemble. All of them have an associated value of the nuclear incompressibility K lying in the interval 210-270 MeV [25]. The original references in which the parameter sets used in the present analysis can be found are [26,27]. The predictions based on relativistic calculations, reported in reference 24, are based on the well-known relativistic mean field (RMF) theory plus the self-consistent relativistic RPA (RRPA) as described in Refs. [28,29]. These relativistic calculations employed 7 different parametrizations for the non-linear, meson-exchange effective Lagrangian.

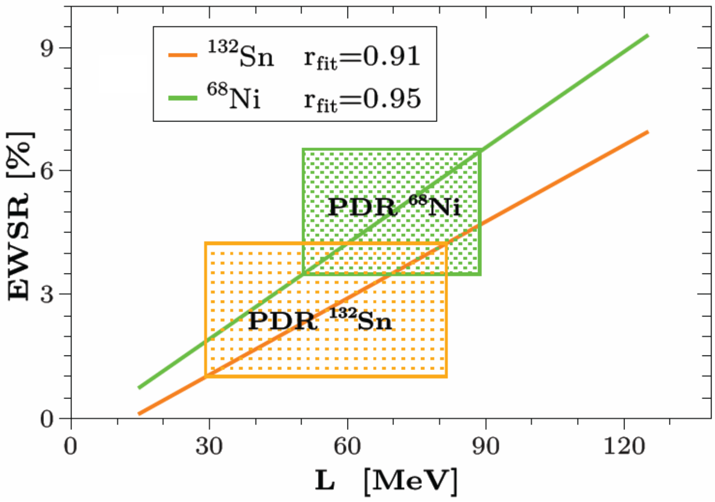

Figure 5. Correlation between fraction on the energy weighted sum rule strength in the region of the pygmy resonance and the value of the derivative of symmetry energy. The line in orange (the lower one in the figure) is for the nucleus ^{132}Sn and the green line (the upper one in the figure) is for the nucleus ^{68}Ni. These lines represent the linear fit of the data calculated using different forces and the corresponding correlation coefficients are given in the legenda. The two squares (the bottom for ^{132}Sn and the top for ^{68}Ni) correspond to the measured values where the vertical size is given by the uncertainty related to the extraction of the energy weighted sum rule values from the experiment.

Firstly the relation between the value of the energy weighted sum rule EWSR in the region of the pygmy resonance and the value of the derivative of the symmetry energy L was examined for all the results of the calculations corresponding to the different forces. A very good correlation has been found between the percentage of the EWSR and L as one can see in figure 5, where the linear fits to the calculated data are shown for both ^{68}Ni and ^{132}Sn nuclei. We have then used the measured values of the EWSR percentage to deduce the corresponding range of acceptable values for L. It should be pointed out that this approach is similar to that of reference 16, although more general because two different nuclei and many different mean field models were considered. In spite of the fact that this analysis does not include all classes of mean field models, possible sources of bias were avoided as much as possible by not restricting to Skyrme sets fitted by the same group with the same protocol. In fact, the used set of forces spans a broad range of possible values associated with nuclear matter quantities.

The present analysis has constrained the slope parameter L to be in the interval 50.3-89.4 MeV or 29.0-82.0 MeV, if we use either the ^{68}Ni results, or the ^{132}Sn results (cf. figure 5). The weighted average is L =64.8±15.7 MeV. As discussed more in detailed in reference 24 the correlation between the symmetry energy at saturation J and derivative of the symmetry energy L was deduced with the best value of J being 32.3±1.3 MeV. This value is in very good agreement with the value 32.0±1.8 MeV which is reported in [16]. The parametrizations of S( ) found in Refs. [30,31] lead to J = 31.6 MeV. Moreover, the present result for J overlaps well with the ranges obtained in Refs. [32] (30.2-33.8 MeV) and [33] (31.5-33.5 MeV) (cf. also [34]). From the theoretical point of view, we can consider very satisfactory that this result for L coincides almost exactly with the value of 66.5 MeV extracted from BrucknerHartree-Fock (BHF) calculations in uniform matter that employ realistic two-body and three-body forces [35].

The next step is to use the L value obtained from the PDR computed data points in ^{68}Ni and ^{132}Sn in order to deduce the neutron skin thickness R.

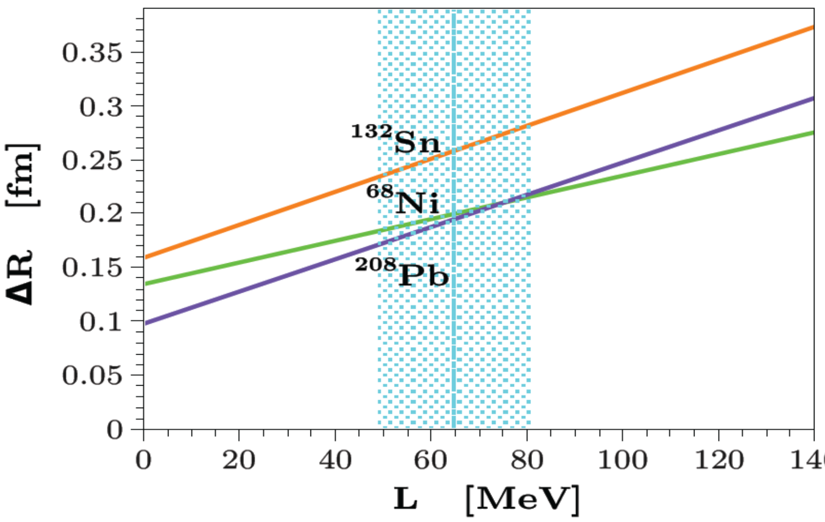

Figure 6. Correlation between the value of the neutron skin thickness R and the value of the derivative of the symmetry energy L. The 3 lines (violet, green and orange being the bottom, medium and upper lines at L=0, respectively) represent the linear fit to the calculations using different forces.
The shaded vertical stripe corresponds to the values of L =64.8±15.7 MeV as deduced from the combined analysis for ^{68}Ni and ^{132}Sn of the correlation between EWSR and L. The deduced values of the neutron skin thickness are R=0.200±0.015 fm for ^{68}Ni, R =0.258±0.024 fm for ^{132}Sn, and R=0.194±0.024 fm for ^{208}Pb.

As displayed in figure 6 the correlation between L and R, when the two quantities are calculated, is found to be quite good. If one imposes the value of L to be in the interval of 64.8±15.7 MeV, one obtains for the skin thickness R=0.200±0.015 fm for ^{68}Ni,
R =0.258±0.024 fm for ^{132}Sn, and R=0.194±0.024 fm for ^{208}Pb. These numbers are stable if one tries to constrain them by using the L value from ^{68}Ni only, or ^{132}Sn only, instead of the weighted average. It should also be noted that the values associated with R, both for ^{132}Sn and ^{208}Pb, are in good agreement with the results reported in Ref. [16]. This gives us further confidence on the value
of the neutron skin of ^{68}Ni which is determined for the first time through the present analysis. We should recall that the possibility to extract R directly from measurements of the spin-dipole strength has been discussed [36]. For a thorough discussion of the exensive literature appeared in
previous decades on this subject we refer the reader to Ref. [37].

The values of L and J found with the present analysis are compared with the results obtained with the analysis of heavy ion collisions for which the experimental isoscaling data exist. In particular the heavy ion collision analysis was made using asymmetric and symmetric collisions involving Sn isotopes (see reference 32). The result of this analysis provides the L and J values lying in the shaded band in figure 7. In the same figure the constrain from the pygmy dipole resonance analysis is given in the bottom box while that obtained from symmetry energy analysis on nuclei (reported in reference 33) is displayed in the top box. One notes that the present finding overlaps significantly with the heavy ion results. In addition, as discussed more in detailed in reference 24 a good overlap is found for the values of L obtained in the present with those deduced with several other methods and analysis.

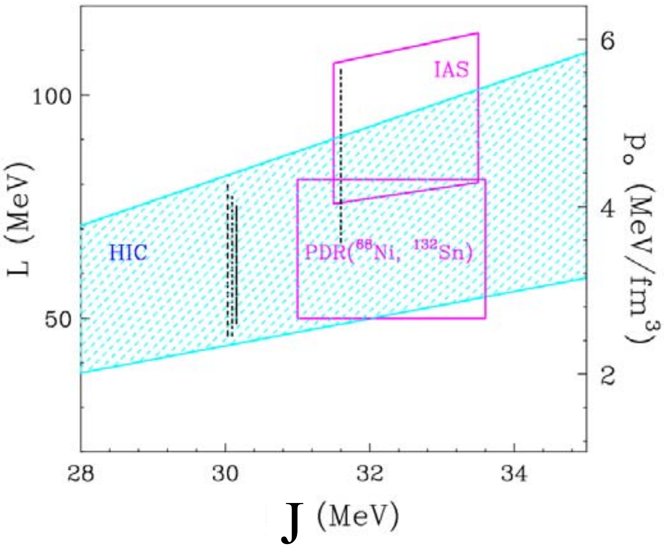

Figure 7. Representation of the constraints on the parameters J and L, namely the symmetry energy at saturation and of the derivative of the symmetry energy. The region bounded by the diagonal lines represents the constraints from the analysis of heavy ion collisions between different Sn isotopes.The right axis corresponds to the neutron matter symmetry pressure at saturation density. The upper box represents the constraints given by the analysis of the symmetry energy from nuclei as reported in reference 33. The lower box is formed by the constraints from the present analysis of the pygmy data on ^{68}Ni and ^{132}Sn.

4. Conclusions

The gamma decay following the Coulomb excitation of the neutron rich ^{68}Ni radioactive beam at 600 MeV/nucleon was measured using the RISING setup. A sizable fraction of "pygmy" dipole strength has been found in this nucleus. A combined analysis of this result together with that obtained by the LAND collaboration for ^{132}Sn was made. This analysis used calculations with different sets of interactions (RPA and RRPA calculations) and has investigated the correlations between the pygmy strength espressesed in EWSR, the derivative of the symmetry energy L and the neutron skin thickness R. Constrains on L are obtained using the experimental data for ^{68}Ni and ^{132}Sn corresponding to reasonable values of the neutron skin thickness R. As compared to a previous work using only relativistic calculations and the result for ^{132}Sn only, this analysis has shown that with more data and with a more general framework the extraction of the slope parameter L is much better constrained. Another important side result of this work is that a value for the neutron skin thickness of the neutron-rich ^{68}Ni isotope was proposed for the first time. More pygmy dipole resonance data in other mass regions and/or in long isotopic chains are desirable to increase the predictive power of this procedure. This could lead to determine quite accurately quantities such as the neutron radii, and the parameters governing the density dependence of the symmetry energy, that are fundamental for nuclear physics and for their implications in the study of neutron stars.

Acknowledgment

I like to express special thanks O. Wieland, F. Camera and G. Colo' for their very important contributions to this work . The other collaborators to be acknowledged are: P.F. Bortignon, A. Carbone, G.Benzoni, N.Blasi, S.Brambilla, F.C.L.Crespi, S.Leoni, B.Million, R.Nicolini, A.Maj, P.Bednarczyk, J.Grebosz, M.Kmiecik, W.Meczynski, J.Styczen, T.Aumann, A.Banu, T.Beck, F. Becker, L.Caceres, P.Doornenbal, H.Emling, J.Gerl, H.Geissel, M.Gorska, O.Kavatsyuk, M.Kavatsyuk, I.Kojouharov, N.Kurz, R.Lozeva, N.Saito, T.Saito, H.Schaffner, H.J.Wollersheim, J.Jolie, P.Reiter, N.Warr, G.de Angelis, A.Gadea, D.Napoli, S.Lenzi, S.Lunardi, D.Balabanski, G.Lo Bianco, C.Petrache, A.Saltarelli, M.Castoldi, A.Zucchiatti, J.Walker, A.Burger.

[1] A. W. Steiner et al., Phys. Rep. **411**, 325 (2005).
[2] C.J. Horowitz and Piekarewicz, Phys. Rev. Lett. **86**, 5647 (2001).
[3] J. Piekarewicz Phys. Rev. **C73**, 044325 (2006).
[4] D. Vretenar et al., Nucl. Phys. **A692**, 496 (2001).
[5] N. Paar et al., Phys. Rev. **C67**, 34312 (2003).
[6] D. Sacchi et al., Phys. Lett. **B601**, 27 (2004).
[7] N Tsoneva et al., Phys. Lett. **B586**, 213 (2004).
[8] A. Zilges et al., Phys. Lett. **B542**, 43 (2002).
[9] S. Volz et al., Nucl. Phys. **A779**, 1 (2006).
[10] N. Ryezayeva et al., Phys. Rev. Lett. **89,** 272502 (2002).
[11] D. Savran et al., Phys. Rev. Lett. **97**, 172502 (2006).
[12] D. Savran et al., contribution to this volume.
[13] A. Leistenschneider et al., Phys. Rev. Lett. **86**, 5442 (2001).
[14] J. Gibelin et al., Phys. Rev. Lett. **101**, 212503 (2008).
[15] P. Adrich et al., Phys. Rev. Lett. **95**, 132501 (2005).
[16] A. Klimkiewicz et al., Phys. Rev. **C76**, 051603(R) (2007).
[17] H. Geissel et al., Nucl. Instr. and Meth. **B70** 286 (1992).
[18] R. Lozeva et al. J.Phy. G: Nucl. Part. Phys. **31 S**1917 (2005).
[19] H.J. Wollersheim et al. NIM **A 537** (2005) 637.
[20] A. Bracco et al., Mod. Phys. Lett. **A22**, 33(2007).
[21] O. Wieland et al., Phys. Rev. Lett. **102**, 092502 (2009).
[22] A. Bracco, Acta Phys. Pol. **B40**, 535(2009).
[23] Y. Alhassid et al., Phys. Rev. Lett. **99**, 162504 (2007); C. N. Gilbreth and Y. Alhassid, private communication.
[24] A. Carbone et al., Phys. Rev. **C81**, 041301R(2010).
[25] S. Shlomo et al., Eur. Phys. J. **A30**, 23 (2006); G. Colo, Phys. of Part. and Nucl. **39**, 286 (2008).
[26] L. Trippa et al., Phys. Rev. **C77**, 061304(R) (2008).
[27] J. R. Stone et al., Phys. Rev. **C68**, 034324 (2003).
[28] P. Ring et al., Nucl. Phys. **A694**, 249 (2001).
[29] Z. Y. Ma et al., Nucl. Phys. **A703**, 222 (2002).
[30] L. W. Chen et al., Phys. Rev. Lett. **94**, 032701 (2005).
[31] D. V. Shetty et al., Phys. Rev. **C76**, 024606 (2007).
[32] M. B. Tsang et al., Phys. Rev. Lett. **102**, 122701 (2009).
[33] P. Danielewicz and J. Lee, Nucl. Phys. **A818**, 36 (2009).
[34] P. Danielewicz, Nucl. Phys. **A727**, 233 (2003).
[35] I. Vida˜na et al., Phys. Rev. **C80**, 045806 (2009).
[36] A. Krasznahorkay et al., Phys. Rev. Lett. **82**, 3216 (1999).
[37] M. N. Harakeh and A. van der Woude, Giant Resonances, (Clarendon Press, Oxoford, 2001).